Circulation Research

ORIGINAL RESEARCH

MIR503HG Loss Promotes Endothelial-to-Mesenchymal Transition in Vascular Disease

João P. Monteiro,* Julie Rodor,* Axelle Caudrillier, Jessica P. Scanlon, Ana-Mishel Spiroski, Tatiana Dudnakova, Beatrice Pflüger-Müller, Alena Shmakova, Alex von Kriegsheim, Lin Deng, Richard S. Taylor, John R. Wilson-Kanamori, Shiau-Haln Chen, Kevin Stewart, Adrian Thomson, Tijana Mitić, John D. McClure, Jean Iynikkel, Patrick W.F. Hadoke, Laura Denby, Angela C. Bradshaw, Paola Caruso, Nicholas W. Morrell, Jason C. Kovacic, Igor Ulitsky, Neil C. Henderson, Andrea Caporali, Matthias S. Leisegang, Ralf P. Brandes, Andrew H. Baker

RATIONALE: Endothelial-to-mesenchymal transition (EndMT) is a dynamic biological process involved in pathological vascular remodeling. However, the molecular mechanisms that govern this transition remain largely unknown, including the contribution of long noncoding RNAs (lncRNAs).

OBJECTIVES: To investigate the role of lncRNAs in EndMT and their relevance to vascular remodeling.

METHODS AND RESULTS: To study EndMT in vitro, primary endothelial cells were treated with transforming growth factor-β2 and interleukin-1β. Single-cell and bulk RNA-seq (RNA-sequencing) were performed to investigate the transcriptional architecture of EndMT and identify regulated lncRNAs. The functional contribution of seven lncRNAs during EndMT was investigated based on a DsiRNA (dicer-substrate short interfering RNAs) screening assay. The loss of lncRNA MIR503HG was identified as a common signature across multiple human endothelial cell types undergoing EndMT in vitro. MIR503HG depletion induced a spontaneous EndMT phenotype, while its overexpression repressed hallmark EndMT changes, regulating 29% of its transcriptome signature. Importantly, the phenotypic changes induced by MIR503HG were independent of miR-424 and miR-503, which overlap the lncRNA locus. The pathological relevance of MIR503HG downregulation was confirmed in vivo using sugen/hypoxia–induced pulmonary hypertension in mice, as well as in human clinical samples, in lung sections and blood outgrowth endothelial cells from pulmonary arterial hypertension patients. Overexpression of human MIR503HG in sugen/hypoxia mice led to reduced mesenchymal marker expression, suggesting MIR503HG therapeutic potential. We also revealed that MIR503HG interacts with the PTBP1 (polypyrimidine tract binding protein 1) and regulates its protein level. PTBP1 regulation of EndMT markers suggests that the role of MIR503HG in EndMT might be mediated in part by PTBP1.

CONCLUSIONS: This study reports a novel lncRNA transcriptional profile associated with EndMT and reveals the crucial role of the loss of MIR503HG in EndMT and its relevance to pulmonary hypertension.

GRAPHIC ABSTRACT: A graphic abstract is available for this article.

Key Words: endothelial cells ■ lncRNA ■ microRNAs ■ pulmonary arterial hypertension ■ vascular remodeling

Meet the First Author, see p 1121

Correspondence to: Andrew H. Baker, PhD, University of Edinburgh, Queen's Medical Research Institute, 47 Little France Crescent, Edinburgh, United Kingdom, EH16 4TJ. Email andy.baker@ed.ac.uk

*J.P. Monteiro and J. Rodor contributed equally

The Data Supplement is available with this article at https://www.ahajournals.org/doi/suppl/10.1161/CIRCRESAHA.120.318124.

For Sources of Funding and Disclosures, see page 1188.

Circulation Research is available at www.ahajournals.org/journal/res

Novelty and Significance

What Is Known?

- Endothelial to mesenchymal transition (EndMT) is a complex process contributing to vessel remodeling during disease, including pulmonary arterial hypertension.
- Long noncoding RNAs (lncRNAs) regulate many biological processes and are involved in vascular biology and disease.

What New Information Does This Article Contribute?

- Transcriptomic changes associated with EndMT include lncRNAs.
- The lncRNA MIR503HG is downregulated during EndMT in vitro, as well as in mouse and human pulmonary arterial hypertension samples.
- Downregulation of MIR503HG level induces a spontaneous EndMT profile which may be mediated, in part, by MIR503HG interaction with the RNA binding protein PTBP1 (polypyrimidine tract binding protein 1).

EndMT transition occurs during development and pathological vessel remodeling. Regulators of EndMT are still poorly characterized. LncRNAs are key regulators of many biological processes and are involved in disease. Here, we identify lncRNAs regulated during EndMT and show that the lncRNA MIR503HG expression is decreased during EndMT in vitro. Loss of MIR503HG was also observed both in mouse and human pulmonary arterial hypertension samples. Downregulation of MIR503HG alone recapitulates EndMT while its overexpression reduces EndMT. MIR503HG mechanism of action was uncovered, by identifying the RNA binding protein PTBP1 as a binding partner and showing PTBP1 regulation of mesenchymal genes. We provide early evidence of MIR503HG therapeutic potential in a mouse model.

Nonstandard Abbreviations and Acronyms

CDH5	cadherin 5
EC	endothelial cell
EndMT	endothelial to mesenchymal transition
HNRNPA0	heterogeneous nuclear ribonucleoprotein A0
HPAEC	human pulmonary artery endothelial cells
HUVEC	human umbilical vein endothelial cells
IL	interleukin
LncRNA	long noncoding RNA
MiRNA/miR	microRNA
PAH	pulmonary arterial hypertension
PH	pulmonary hypertension
PTBP1	polypyrimidine tract binding protein 1
RNA-seq	RNA sequencing
SuHx	Sugen/Hypoxia
TGF	transforming growth factor

Endothelial to mesenchymal transition (EndMT) is a complex cellular transdifferentiation process whereby endothelial cells (EC) lose their endothelial identity and acquire mesenchymal cell characteristics.[1] Akin to epithelial-to-mesenchymal transition, EndMT has been described during heart embryonic development,[1] as well as in neovascularization and tissue repair.[2] Although its role remains under debate, EndMT has been shown to be involved in a variety of maladaptive tissue remodeling scenarios,[3–6] such as atherosclerosis[7] and vein graft remodeling.[8] Such remodeling is also causal in pulmonary arterial hypertension (PAH), a progressive disease with limited treatment options, largely defined by structural alterations to the lung vasculature. These alterations include stiffening of proximal pulmonary arteries, increased intimal and medial arterial thickness, along with the eventual development of complex neointimal lesions. Underlying many of these changes is the increased deposition of extracellular matrix and appearance of smooth muscle–like cells with high proliferative and migratory potential.[9] Several reports now suggest the involvement of EndMT during both the development and progression of PAH, opening new therapeutic avenues.[10–12] As both PAH and EndMT are linked with imbalance in TGF (transforming growth factor)-β signaling, several in vitro models have been developed relying on TGF-β signaling as the main inducer of EndMT, alone, or with an additional stimulus.[7,13]

EndMT is characterized by the decrease of endothelial markers such as PECAM1 (platelet endothelial cell adhesion molecule-1)/CD31 and VE (vascular endothelial)-cadherin/CDH5 (cadherin 5) in association with the gain of mesenchymal markers such as ACTA (α-smooth muscle actin) 2, CNN (calponin) 1,[1] as well as enhanced collagen production. EndMT is also associated with increased expression of several transcription factors such as TWIST (twist-related protein 1), SMAD3 (SMAD family member 3), SNAI1 (snail family transcriptional repressor 1), and SNAI2.[1] However, the precise molecular mechanisms and upstream determinants governing this transition remain to be rigorously defined, particularly when considering

vascular heterogeneity and the presence of distinct stages of EndMT. Indeed, cells that have lost EC markers and thus undergone a complete EndMT process showed high proliferative and migratory capacity whereas partial EndMT cells, still expressing EC markers, have also been isolated.[12] Although both protein-coding genes and microRNAs (miRNAs) have been widely involved in EndMT regulation,[1,14] the role of long noncoding RNAs (lncRNAs) is yet to be thoroughly explored. LncRNAs are long (>200) noncoding transcripts, often expressed at low levels but with high specificity. Several lncRNAs have been described as critical regulators of gene expression both at the transcriptional and post-transcriptional level and have roles in a wide range of diseases.[15] LncRNAs have already been associated with EC function and dysfunction.[16] The lncRNA MALAT1 (metastasis-associated lung adenocarcinoma transcript 1) has been implicated in the modulation of TGF-β1–induced EndMT through regulation of the *miR-145*-TGFBR2 (TGF-beta receptor 2)/SMAD3 axis.[17] Recently, the lncRNA GATA6-AS (antisense transcript of GATA6) was shown to suppress TGF-β2-induced EndMT in vitro via targeting LOXL2 (lysyl oxidase homolog 2).[18]

Here, we have applied an unbiased approach using single-cell and bulk RNA-seq (RNA-sequencing) of an in vitro model of EndMT to characterize EndMT transcriptional changes. We identified 103 differentially expressed lncRNAs during EndMT progression in both venous and arterial ECs. Among these lncRNAs, the substantive loss of the lncRNA MIR503HG was a consistent molecular event during EndMT, both in vitro and in vivo mouse and human samples. We further showed a direct contribution of MIR503HG on the regulation of EndMT, reporting large transcriptional changes and preliminary data on its therapeutic potential.

METHODS

Data Availability

The authors declare that all methods, material list, and processed experimental data are available within the article and its Data Supplement. Any additional data are available from the corresponding author upon request. Raw and processed sequencing data are available at GEO database (accession: GSE118446, GSE118815, GSE159843). All methods are included in the Data Supplement. Please see the Major Resources Table in the Data Supplement for material list.

RESULTS

Induction of EndMT in Arterial and Venous ECs Using TGF-β2 and IL-1β

To replicate EndMT in vitro and characterize its molecular signature, human primary venous (human umbilical vein endothelial cells [HUVEC]) and arterial (human pulmonary artery endothelial cells [HPAEC]) ECs were subjected to a combination of TGF-β2 and IL (interleukin)-1β for 7 days.[13] Real-time quantitative polymerase chain reaction (RT-qPCR) analysis confirmed EndMT induction in TGF-β2 and IL-1β cotreated cells, but not TGF-β2 or IL-1β alone, with the loss of the endothelial marker PECAM1, gain of mesenchymal markers ACTA2 (α-smooth muscle actin 2) and COL1A1 (Collagen Type I Alpha 1 Chain), and the EndMT-associated transcription factor SNAI2 (Figure 1A and Figure IA in the Data Supplement). In addition, changes to PECAM1 and SNAI2 expression were confirmed at the protein level by immunofluorescence microscopy (Figure 1B and Figure IB in the Data Supplement). We also confirmed the decrease of PECAM1 and increase of ACTA2 protein levels by Western blot in HPAEC (Figure IC in the Data Supplement). We also assessed the effect of the TGF-β2 and IL-1β cotreatment on the proliferative and migratory capacities of HUVEC and observed a significant decrease of cellular proliferation (Figure 1D) but no significant change in the migratory capacity of EndMT cells (Figure 1E).

Together, these results confirm the induction of an EndMT-like profile in both arterial and venous EC using a TGF-β2 and IL-1β cotreatment model.

Transcriptional Profiling of Primary ECs Undergoing EndMT

To characterize EndMT transitioning populations and transcriptomic changes associated with this transition, we carried out single-cell RNA-seq on cotreated and control HUVEC at day 0, day 3, and day 7 using 10X Genomics technology. Based on tSNE (t-distributed stochastic neighbor embedding) dimensionality reduction, we confirmed the clear separation between control and TGF-β2 and IL-1β cotreated cells (Figure 2A). Although day 3 and day 7 untreated cells showed some overlap, day 7 treated cells clustered separately from day 3 treated cells showing a time-dependent effect of the treatment (Figure 2A). The loss of an endothelial signature was confirmed using PECAM1, CDH5, ICAM2, ERG, and VWF and the gain of a mesenchymal/ EndMT signature using TAGLN (Transgelin), COL1A1, and S100A4 and SNAI2 expression (Figure 2B). Eleven clusters were identified (Figure 2C), with clusters 1 to 6 corresponding to control HUVEC and displaying an endothelial transcriptional program, whereas clusters 7 to 11 from cotreated HUVEC displayed a downregulation of endothelial genes and progression to a mesenchymal signature (Figure 2D). In agreement with the decrease of proliferation described above (Figure 1D), we observed a decrease of MKI67 expression in groups 8 to 11 (Figure 2D). Cluster 11, composed exclusively from day 7 cotreated HUVEC, constituted a new advanced EndMT population (Figure 2D). Cluster 11 was characterized by the expression of 132 marker genes, including known EndMT markers (TGFBR1, NOTCH2, and BMP2) and novel genes

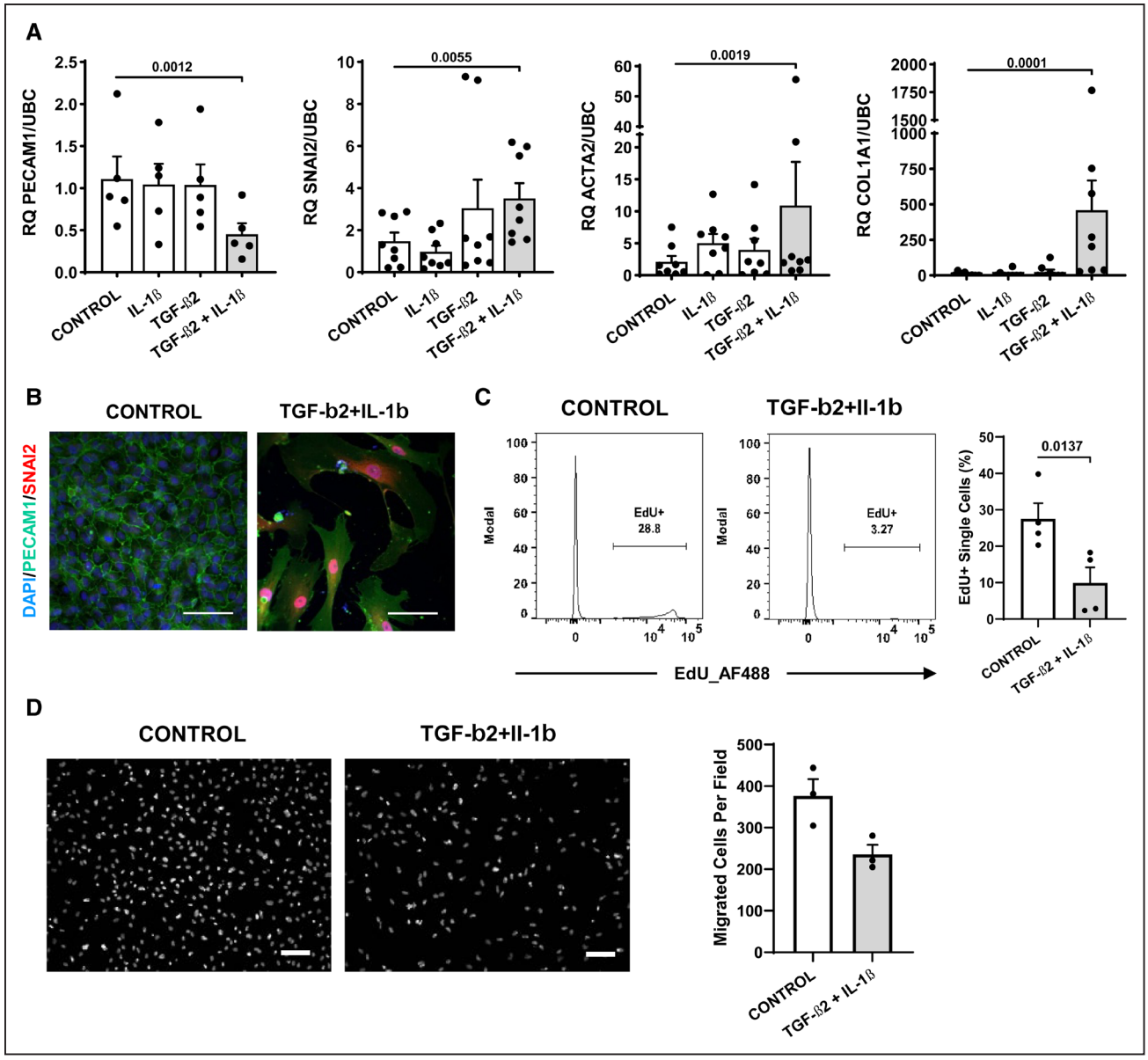

Figure 1. Endothelial-to-mesenchymal transition (EndMT) in vitro model in venous endothelial cell (EC). human umbilical vein ECs (HUVEC) were treated with TGF (transforming growth factor)-β2 (10 ng/mL) and/or IL (interleukin)-1β (1 ng/mL) for 7 d. **A**, Expression analysis of EndMT markers by real-time quantitative polymerase chain reaction relative to UBC (Ubiquitin C) (relative quantification [RQ]). *PECAM1* (platelet endothelial cell adhesion molecule-1) n=5, ACTA2 (α-smooth muscle actin 2), SNAI2 (Snail family transcriptional repressor 2), and COL1A1 (collagen type I alpha 1 chain) n=8. Statistical analysis was done using a repeated-measures 1-way ANOVA with Bonferroni correction. **B**, Representative images of immunofluorescence staining for PECAM1 (green), SNAI2 (red), and DAPI (4′,6-diamidino-2-phenylindole) (blue; scale bar 50 μm). **C**, Quantification of EdU (5-ethynyl-2'-deoxyuridine) uptake in untreated and treated HUVECs (n=4) with representative fluorescence-activated cell sorting (FACS) histogram plots. **D**, Transwell migration assay of treated and untreated HUVECs with representative image of fixed migrated cells stained with DAPI (scale bar 100 μM) and quantification (n=3). Statistical analysis of **C** and **D** was done using linear mixed-effects modeling.

involved in cell differentiation (ANKRD1, OSGIN2) and stress signaling (CXCL8 and CSF3; Figure IIA and IIB in the Data Supplement).

To identify the complete transcriptomic changes associated with EndMT, including lncRNAs, we performed high-depth bulk RNA-seq of HUVEC and HPAEC undergoing EndMT after 7 days (Figure 2, Figure IIIA in the Data Supplement). Principal component analysis confirmed a clear segregation of the different treatment groups, compared with untreated controls (Figure 2E, Figure IIIB in the Data Supplement). HUVEC and HPAEC derived EndMT cells clustered separately not only from their respective control group but also from each other, suggesting transcriptional heterogeneity in the induction of EndMT across vascular beds (Figure 2E, Figure IIIB in the Data Supplement). We identified 1721 upregulated and 1260 downregulated genes in EndMT-HUVEC compared with untreated cells (Dataset I in the Data Supplement), with 46% of the upregulated and 60% of the downregulated genes not observed in the single-treatment groups (Figure 2F, Figure

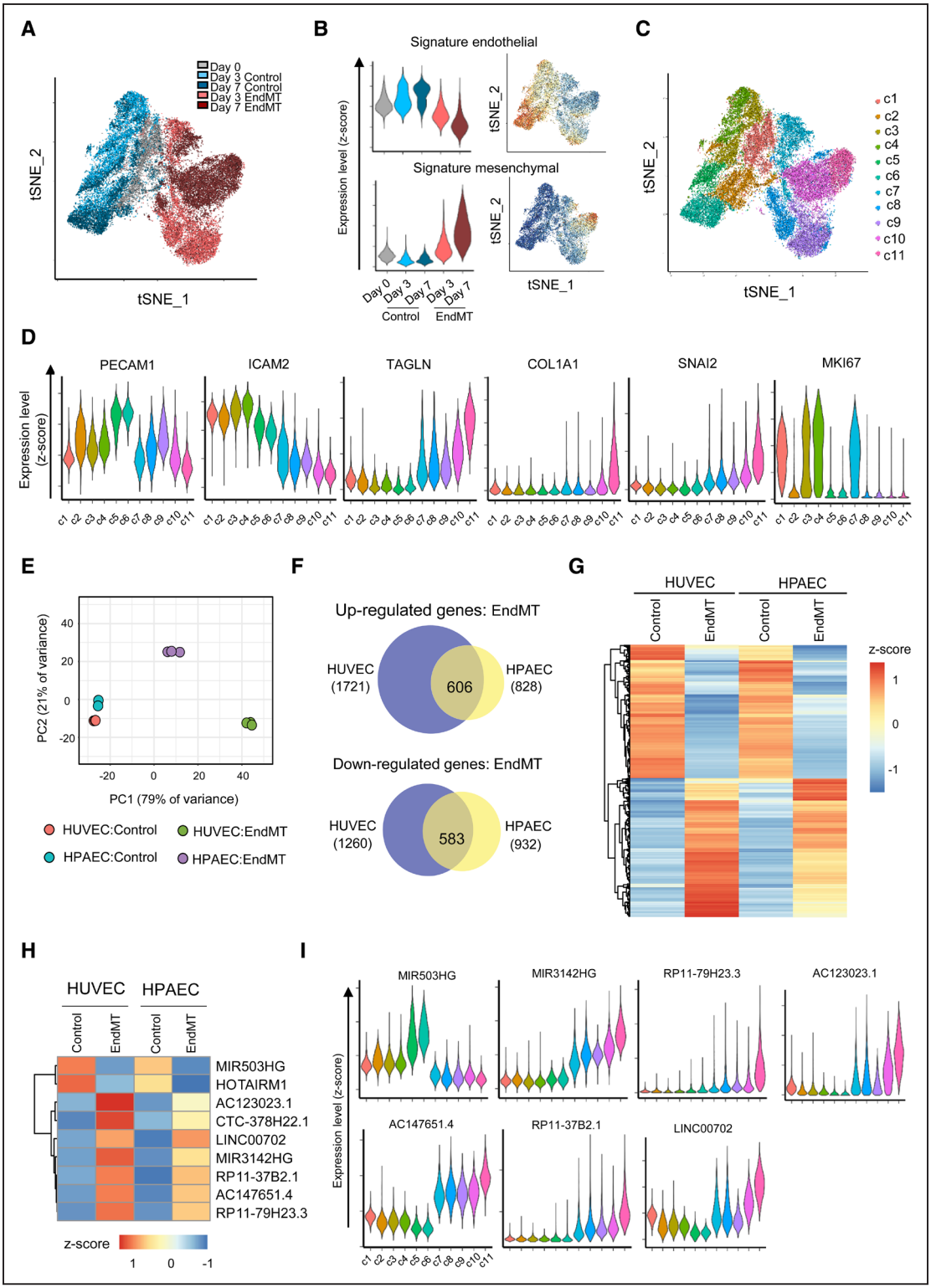

Figure 2. Single-cell and bulk RNA-seq (RNA-sequencing) analysis of endothelial-to-mesenchymal transition (EndMT) identify a common long noncoding RNA (lncRNA) signature.

A, tSNE (t-distributed stochastic neighbor embedding) plot of the 5 datasets (untreated human umbilical vein endothelial cells [HUVEC] at day 0, 3, and 7 and TGF (transforming growth factor)-β2+IL (interleukin)-1β cotreated HUVEC at day 3 and day 7). **B**, Violin and tSNE plots of endothelial and mesenchymal signature. **C**, Unsupervised cluster identification. **D**, Violin plot of endothelial (PECAM1 [platelet endothelial cell adhesion molecule-1], ICAM2 [intercellular adhesion molecule 2]), mesenchymal (TAGLN [Transgelin], COL1A1 [Collagen type I alpha 1 chain]), EndMT (SNAI2 [Snail family transcriptional repressor 2]), and proliferation (MKI67 [Marker of proliferation Ki-67]) marker expression (as *Z* score) in the different clusters. **E**, Principal Component Analysis (PC) of control and EndMT-induced HUVEC and human pulmonary artery endothelial cells (HPAEC; bulk RNA-seq). **F**, Overlap of EndMT up/downregulated genes between HUVEC and HPAEC. **G**, Heatmap of significantly regulated genes and **(H)** of candidate lncRNAs expression (as *Z* score). **I**, Violin plot of candidate lncRNA expression in the single-cell RNA-seq clusters.

IIIC and IIID in the Data Supplement). Importantly, around 40% of regulated genes in HUVECs were also affected in HPAEC (Figure 2F and 2G and Dataset I in the Data Supplement). Gene Ontology analysis found that upregulated genes associated with immune response, whereas downregulated genes associated with Gene Ontology terms related to DNA conformation and cell cycle (Figure IIIE and Dataset II in the Data Supplement).

LncRNA expression was affected upon EndMT induction, with 69 lncRNAs upregulated and 34 downregulated in HUVEC and HPAEC (Dataset I in the Data Supplement). Top lncRNA candidates were selected based on fold change, level of expression, and genomic location: MIR503HG, HOTAIRM1, AC123023.1, CTC-378H22.1, LINC00702, MIR3142HG, RP11-37B2.1, AC147651.4, and RP11-79H23.3 (Figure 2H and Figure IVA and IVB in the Data Supplement). Differential expression patterns were confirmed by RT-qPCR in HUVEC and HPAEC (Figure IVC and IVD in the Data Supplement) for all candidate lncRNAs except CTC-378H22.1 and HOTAIRM1, which failed validation and were removed from downstream analysis (Figure IVA and IVB in the Data Supplement). Using the single-cell RNA-seq dataset, we confirmed the expression changes of all candidates in the advanced EndMT population (Figure 2I). Interestingly, the change for some candidates, including MIR503HG, was also observed in the day 3 sample clusters (Figure 2I) suggesting a role in the early phase of the transition.

Screening for lncRNA Function During EndMT

A short interfering RNA (siRNA)-mediated knockdown approach was utilized to screen the functional contribution of each lncRNA to EndMT (Figure V in the Data Supplement) based on the expression of defined EndMT markers (ie, PECAM1, ACTA2, SNAI2, COL1A1). Significant knockdowns were confirmed for 4 lncRNAs but not for LINC00702, AC147651.4, and AC123023.1, which were subsequently eliminated from this study (Figure VA in the Data Supplement). Targeted depletion of the selected lncRNA candidates lead to significant changes in EndMT markers, highlighting their potential causal contribution to EndMT (Figure VB in the Data Supplement). Notably, knockdown of MIR503HG induced a robust EndMT profile, even in the absence of TGF-β2 and IL-1β cotreatment (Figure VA and VB in the Data Supplement) and as such was chosen for further analysis.

Loss of MIR503HG Is a Common Feature of EndMT In Vitro

MIR503HG is an intergenic lncRNA located on chromosome X with 5 reported isoforms on GENCODE. v26 (Figure 3A and Figure VIA in the Data Supplement). Although RNA-seq data showed a significant downregulation of all isoforms (Figure VIB in the Data Supplement), we confirmed the downregulation of the top 3 expressed isoforms 2, 3, and 5 by RT-qPCR following EndMT induction in HUVEC (Figure VIB and VIC in the Data Supplement). Importantly, as the *MIR503HG* gene locus overlaps with the *miR-424* and *miR-503* genes (Figure 3A), we analyzed their expression during EndMT and observed a significant downregulation of both miR-424-5p and miR-503-5p (Figure 3B).

Interestingly, the final 595 base-pair region of isoform 2 (MIR503HG_2) is highly conserved based on PhyloP score (Figure VIA in the Data Supplement), as was its secondary substructure.[19] As such, we chose MIR503HG_2 as our main transcript of interest. In addition to HUVEC and HPAEC (Figure IVC and IVD in the Data Supplement), downregulation of MIR503HG_2 after TGF-β2 and IL-1β costimulation was also seen in human saphenous vein ECs (HSVEC) and human coronary artery ECs (HCAEC; Figure 3C). Additionally, MIR503HG_2 expression was decreased in a second in vitro model of EndMT using TGF-β2 and H_2O_2 costimulation[7] (Figure 3D). Using our single-cell RNA-seq data, we also confirmed the positive correlation of MIR503HG with the EC signature and a negative correlation for mesenchymal signature (Figure 3E).

As subcellular localization of lncRNA can provide information regarding function, MIR503HG localization was determined by RT-qPCR of nuclear/cytoplasmic fraction (Figure 3F) and RNA-FISH (Figure 3G) in HUVEC. Together, this data revealed that MIR503HG is predominantly localized to the nucleus, with a mean of 2.16 copies per nuclei (Figure 3G).

Loss of MIR503HG Initiates EndMT in the Absence of TGF-β2 and IL-1β

The siRNA screening approach was validated on a larger sample size. We confirmed that all expressed MIR503HG isoforms were downregulated in the si503HG (siRNA-mediated MIR503HG depleted) samples (Figure VIIA in the Data Supplement) and that, in the absence of treatment, si503HG induces an EndMT profile based on RT-qPCR analysis (Figure 4A and 4B). These effects were mirrored at the protein level based on immunofluorescence (Figure 4C) and Western blot (VIIB in the Data Supplement). Furthermore, we showed that MIR503HG depletion not only replicated the key phenotypes of the EndMT model, such as loss of EC monolayer integrity (Figure 4C) and decreased proliferation (Figure VIIC in the Data Supplement), but also showed a decrease in cell migration (Figure VIID in the Data Supplement).

Given the nuclear localization of MIR503HG, an antisense GapmeR (locked nucleic acid oligonucleotide) (gap503HG) was also used to manipulate MIR503HG expression (Figure VIIIA in the Data Supplement) and replicated the findings of the siRNA-mediated knockdown, inducing similar expression

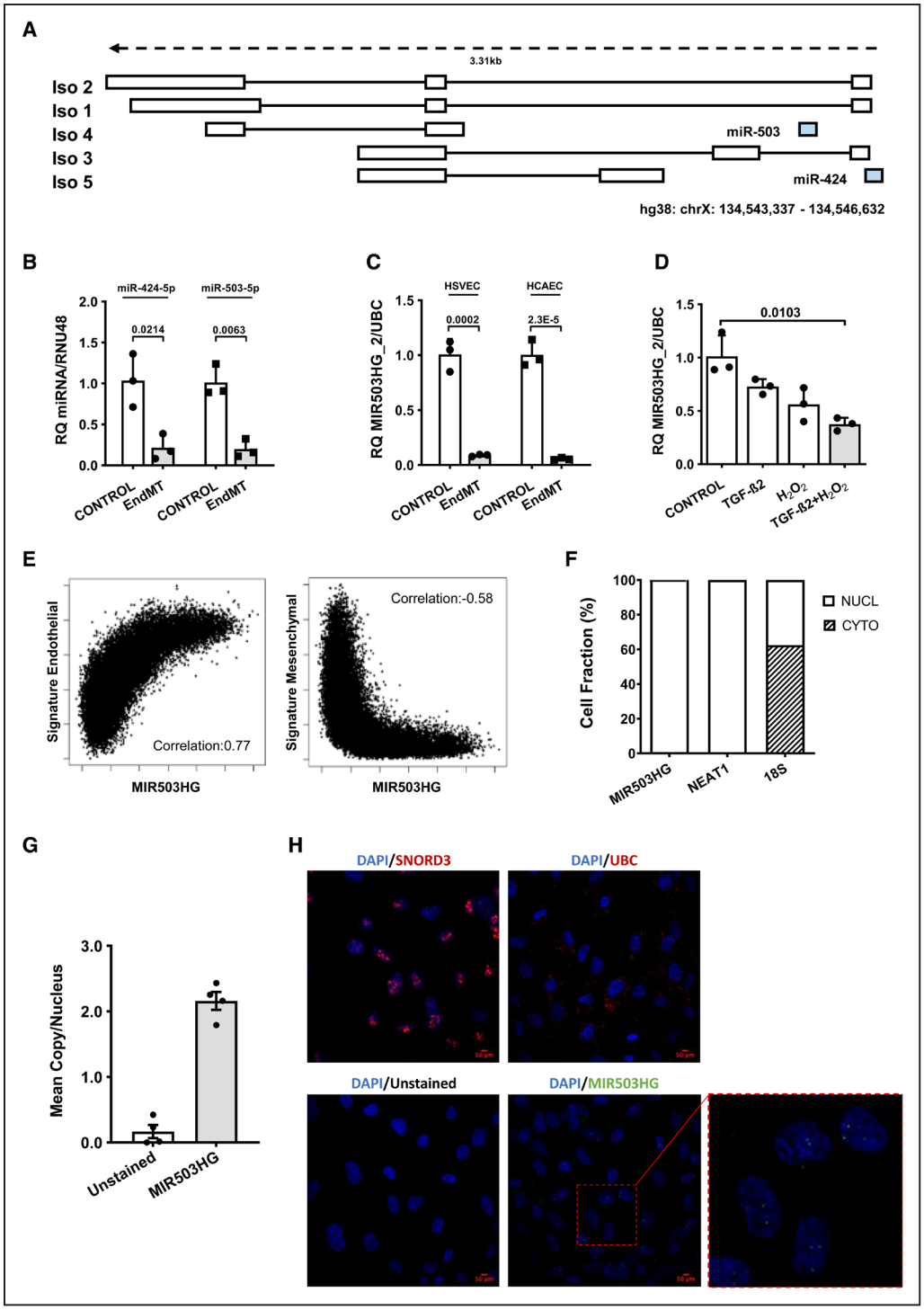

Figure 3. MIR503HG expression during endothelial-to-mesenchymal transition (EndMT) in vitro.
A, Schematic representation of the *MIR503HG*, *miRNA-424,* and *miRNA-503* loci based on GENCODE v26 annotation. **B**, Expression of miRNA-424/-503 in human umbilical vein endothelial cells (HUVEC)±EndMT (TGF [transforming growth factor]-β2+IL [interleukin]-1β; n=4). **C**, MIR503HG_2 expression in HSVEC and HCAEC±EndMT (n=3). **D**, MIR503HG_2 expression in HUVEC after treatment with TGF-β2 (50 ng/mL) and H_2O_2 (200 nM; n=3). **E**, MIR503HG correlation to endothelial and mesenchymal signatures based on single-cell (RNA-sequencing). **F**, MIR503HG_2, 18S, and NEAT1 (Nuclear Enriched Abundant Transcript 1) localization by cell fractionation. **G**, Mean MIR503HG nuclear copy number compared to unstained negative control (n=4) (**H**) and localization of MIR503HG, SNORD3 (Small nucleolar RNA, C/D box 3 cluster), and UBC (Ubiquitin C) by RNA-fluorescence in situ hybridization (FISH) in HUVEC. Relative quantification of real-time quantitative polymerase chain reaction normalized to RNU48 or UBC relative to control cells. Statistical analysis was done using linear mixed-effects modeling for **B** and **C** or a repeated-measures 1-way ANOVA with Bonferroni correction for **D**. chrX indicates X chromosome; CYTO, cytoplasmic; HCAEC, human coronary artery EC; hg, homo sapiens genome assembly; HSVEC, human saphenous vein EC; ISO, Isoform; miR/miRNA, microRNA; NUCL, nuclear; and RQ, relative quantification.

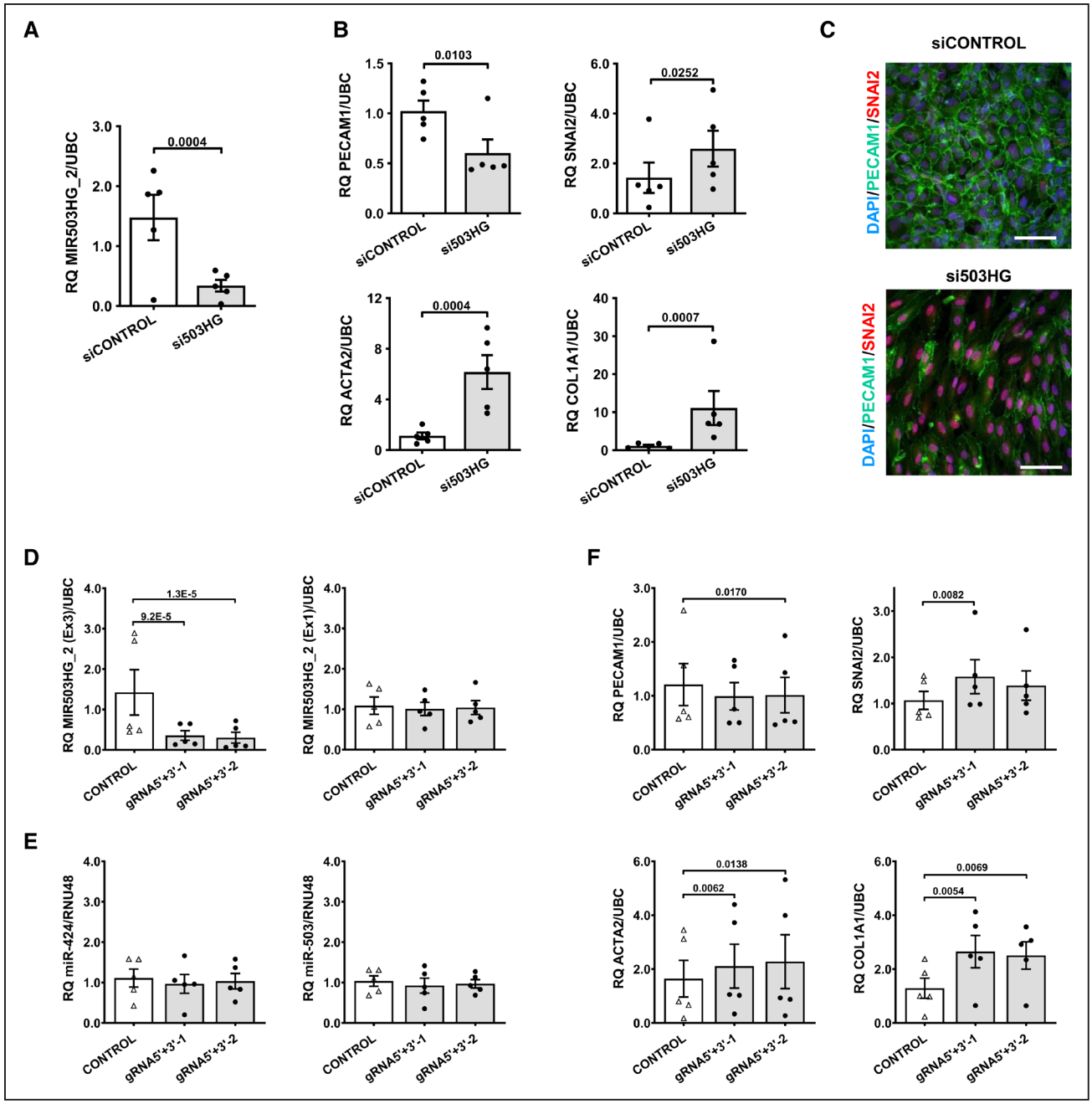

Figure 4. MIR503HG knockdown induces endothelial-to-mesenchymal transition (EndMT) in human umbilical vein endothelial cells (HUVEC).

A, MIR503HG_2 expression in siRNA-mediated MIR503HG depletion (si503HG [siRNA-mediated MIR503HG depleted]) after 7 d in HUVEC (n=3). **B**, EndMT marker gene expression in si503HG compared with control (siControl) after 7 d (n=3). **C**, Representative immunofluorescence images of EndMT markers expression in HUVEC (scale bar 50 μm) after knockdown using si503HG. PECAM1 (platelet endothelial cell adhesion molecule-1; green), SNAI2 (Snail family transcriptional repressor 2; red) (red) and DAPI (4′,6-diamidino-2-phenylindole; blue) (blue). **D**, MIR503HG_2 (**left**: CRISPR/Cas9–targeted Exon3 [Ex3], **right**: untargeted Exon1 [Ex1]), **(E)** miR-424 and miR-503, and **(F)** EndMT marker gene expression in HUVECs following CRISPR-mediated deletion of *MIR503HG,* using 2 lentiviral CRISPR/Cas9 gRNA (guide RNA) pairs, after 8 d compared to empty control pairs (n=5). Relative quantification of real-time quantitative polymerase chain reaction normalized to RNU48 or UBC (Ubiquitin C) relative to Control cells. Statistical analysis was done using linear mixed-effects modeling for **A** and **B** and a repeated-measures 1-way ANOVA with Bonferroni correction for **D**–**F**. ACTA indicates α-smooth muscle actin; COL1A1, collagen type I alpha 1 chain; and RQ, relative quantification.

changes to EndMT markers at the RNA (Figure VIIIB in the Data Supplement) and protein levels (Figure VIIIC in the Data Supplement).

We observed a significant reduction in the expression of miR-424 and miR-503 with siRNA but not GapmeR-mediated MIR503HG depletion (Figure IX in the Data Supplement), presumably due to the oligonucleotides targeting the miRNA precursor. To target specifically MIR503HG, we used a lentiviral CRISPR/Cas9 gene-editing system to delete the conserved exon of

MIR503HG locus without disturbing the miRNA cluster upstream. Cotransduction of HUVEC using 2 separate lentiviral CRISPR/Cas9 gRNA (guide RNA) pairs, led to a >50% reduction in the expression of the target region (exon 3; Figure 4D) while maintaining *miR-424* and *miR-503* as well as *MIR503HG* exon 1 expression after 8 days (Figure 4D and 4E). As with our previous knockdown strategies, reduced MIR503HG availability in HUVEC resulted in similar changes to EndMT marker expression (Figure 4F). Of note, for one of the guide combinations, no statistical difference was observed for PECAM1 and SNAI2 expression. Finally, an anti-miR strategy was used to interrogate the direct contribution of miR-503 and miR-424 to EndMT in HUVEC. Knocking down either miR-503 and miR-424 (Figure XA in the Data Supplement) had no significant effect on the expression level of MIR503HG (Figure XB in the Data Supplement). Moreover, EndMT was not induced by knockdown of either miRNA, with no statistical difference in endothelial or mesenchymal markers observed (Figure XC in the Data Supplement). These data showed that the role of MIR503HG on EndMT regulation is independent of miR-503 and miR-424.

Overexpression of MIR503HG Isoform 2 Represses EndMT

To assess if MIR503HG overexpression could prevent EndMT, we designed a lentiviral vector carrying the MIR503HG_2 transcript sequence (LNT_503HG). HUVEC were transfected with LNT_503HG or lentivirus control (LNT_CT). At 3 days post-transduction, LNT_503HG samples showed an increase of MIR503HG_2 only and not isoforms 3 and 5, when compared with LNT_CT (Figure XIA in the Data Supplement). Cellular fractionation and RNA-FISH confirmed the predominant nuclear localization of overexpressed MIR503HG, with a mean number of 6.46 copies per nuclei (Figure XIB through XID in the Data Supplement). Overexpression of MIR503HG (Figure 5A) did not affect expression of endothelial or mesenchymal markers under control conditions (Figure 5B). However, under EndMT conditions, MIR503HG overexpressing cells (Figure 5A) showed an increase in PECAM1 expression and a marked suppression of SNAI2 and COL1A1 expression compared with LNT_CT (Figure 5B). Immunofluorescence validated these results at the protein level (Figure 5C). Overexpression of MIR503HG did not affect miR-424 or miR-503 levels compared with LNT_CT, in either control or EndMT conditions (Figure XII in the Data Supplement), further confirming a miRNA-independent role of MIR503HG on EndMT.

To identify the contribution of MIR503HG overexpression on the EndMT transcriptomic changes, we performed RNA-seq on control and EndMT-HUVEC with lentiviral overexpression (Dataset III in the Data Supplement). Principal component analysis revealed that LNT_503HG_2 had no major effect on the transcriptome of untreated cells (Control_LNT_503HG_2), clustering with Control and Control_LNT_CT cells (Figure XIII in the Data Supplement). Interestingly, EndMT_LNT_503HG cells clustered in between Control and EndMT cells (Figure XIII in the Data Supplement), suggesting the treatment with LNT_503HG is preventing the EndMT process. We identified 803 and 880 genes upregulated and downregulated, respectively, by MIR503HG overexpression in EndMT (EndMT_LNT_503HG compared with EndMT_LNT_CT; Figure 5D). We found a 29% overlap between EndMT regulated genes and the genes regulated by LNT_503 in treated conditions (Figure 5E). These overlapping genes include additional markers of EndMT such as the endothelial genes NR2F2 and NOS3 as well as the mesenchymal genes TAGLN, FN1, and CNN1. This data again confirms the strong contribution of MIR503HG to EndMT.

MIR503HG Expression Is Lost During Vascular Remodeling in a Mouse Pulmonary Hypertension Model

To examine the contribution of MIR503HG in vivo, we used a sugen/hypoxia (SuHx) pulmonary hypertension (PH) mouse model, in which vessel remodeling involves EndMT[10] (Figure 6A). Additionally, we used an inducible endothelial lineage tracing system of Ind.Endotrack (Cdh5-CreER^{T2}-TdTomato) mice,[20,21] in which TdTomato is constitutively expressed after Tamoxifen treatment in all EC regardless of subsequent changes in cellular phenotype.[8] Ind.Endotrack mice were subjected to SuHx or control conditions for 3 weeks. TdTomato$^+$ cells isolated from SuHx lungs presented an EndMT profile with increased expression of mesenchymal-specific markers (Acta2, Vimentin and Col1a1, Snai2) and loss of endothelial specificity (Pecam1 and Cdh5) when compared with control mice (Figure 6B). Notably, expression of the MIR503HG mouse homolog, Gm28730 (locus and primers shown in Figure XIV in the Data Supplement), was found to be significantly reduced in SuHx TdTomato$^+$ EC (Figure 6C).

To establish the role of MIR503HG in EndMT in vivo, we overexpressed the human MIR503HG_2 transcript in mice and assessed its impact on the EndMT markers after PH induction. We optimized the uptake of a GFP (green fluorescent protein) lentiviral construct on normoxic mice, using intranasal delivery. Flow cytometry analysis confirmed the presence of GFP$^+$ cells in the lung, 13.7% of which corresponded to CD31$^+$ ECs (Figure XVA in the Data Supplement). This delivery protocol was utilized to deliver either LNT_503HG or LNT_CT to 8- to 10-week-old C57BL/6 mice, which then underwent PH induction by SuHx (Figure 6D). Endothelial (CD31$^+$) and CD31$^-$ lung cells were isolated by flow cytometry (Figure XVB in the Data Supplement), and the expression of MIR503HG and EndMT markers was assessed. Human MIR503HG_2 expression was upregulated in

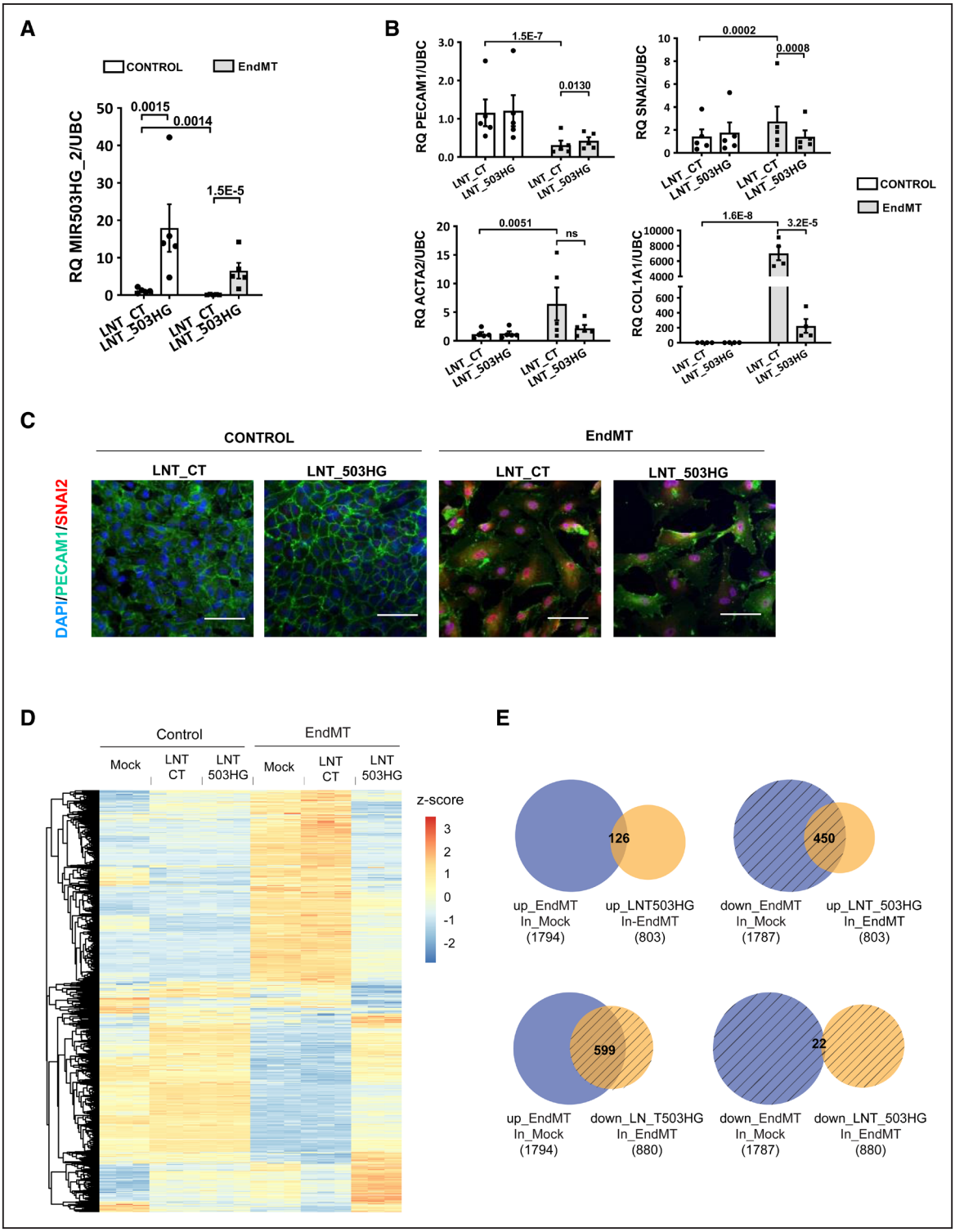

Figure 5. MIR503HG overexpression represses endothelial-to-mesenchymal transition (EndMT) in vitro.
Expression of **(A)** MIR503HG_2 and **(B)** EndMT marker genes in human umbilical vein endothelial cells (HUVEC) following MIR503HG overexpression with lentivirus (LNT)_503HG (multiplicity of infection [MOI] 5) with or without TGF (transforming growth factor)-β2 and IL (interleukin)-1β treatment (Control/EndMT) for 7 d (n=5). Relative quantification of real-time quantitative polymerase chain reaction normalized to UBC (Ubiquitin C) relative to lentivirus control (LNT_CT) in control cells. Analysis by 2-way ANOVA with Bonferroni correction. **C,** Representative immunofluorescence images of EndMT markers in HUVEC following MIR503HG overexpression. PECAM1 (platelet endothelial cell adhesion molecule-1; green), SNAI2 (red), and SNAI2 (Snail family transcriptional repressor 2; red), and DAPI (4′,6-diamidino-2-phenylindole; blue (blue; scale bar 50 μm). **D,** Heatmap of the 1683 significant genes between LNT_503HG and LNT_CT in EndMT conditions (displayed as z score). **E,** Venn diagram of the overlap between significant changes due to MIR503HG overexpression in EndMT cells (EndMT_LNT_503HG vs EndMT_LNT_CT) and EndMT changes (EndMT vs Control). ACTA indicates α-smooth muscle actin; COL1A1, collagen type I alpha 1 chain; ns, non-significant; and RQ, relative quantification.

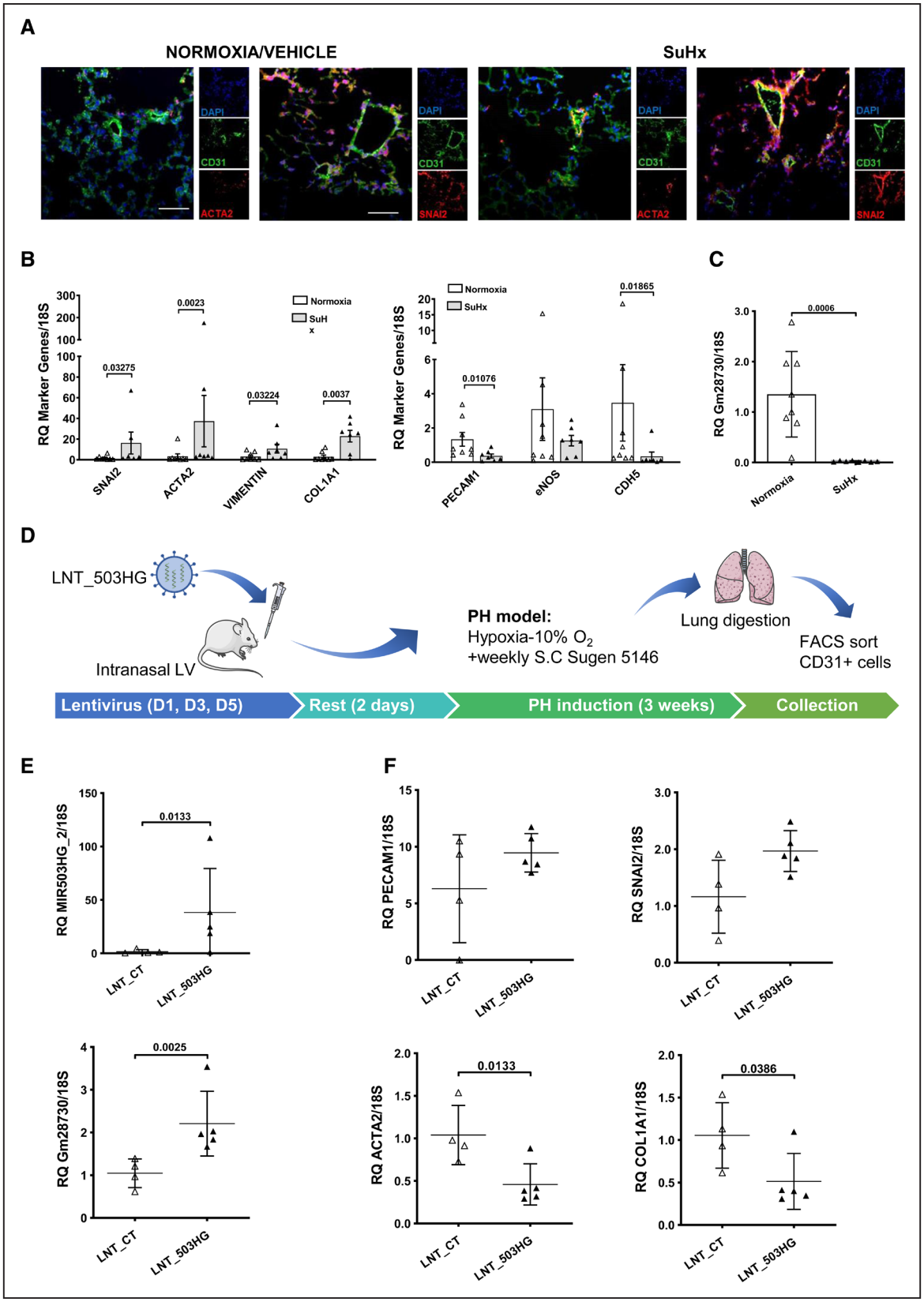

Figure 6. MIR503HG modulation in mice is associated with endothelial-to-mesenchymal transition (EndMT) in pulmonary arterial hypertension (PAH).

A, Representative immunofluorescence staining of normoxia/vehicle or sugen/hypoxia (SuHx) mouse lung tissue for Cd31 (green), DAPI (4′,6-diamidino-2-phenylindole; blue) (blue), and Acta2 (α-smooth muscle actin 2) or Snai2 (Snail family transcriptional repressor 2; red; scale bar 50 μm). **B**, Endothelial and mesenchymal markers expression in TdTomato+ cells isolated from normoxia/vehicle (n=8) or SuHx mouse lung tissue (n=7). **C**, MIR503HG mouse long noncoding RNA (lncRNA) (*Continued*)

both CD31⁻ and CD31⁺ lung cells for LNT_503HG mice compared to LNT_CT (Figure 6E and Figure XVIA in the Data Supplement). The mouse MIR503HG homolog was also increased in LNT_503HG versus LNT_CT CD31⁺ ECs (Figure 6E). Importantly, analysis of EndMT markers revealed the significant downregulation of the mesenchymal markers Acta2 and Col1a1 in LNT_503HG versus LNT_CT CD31⁺ ECs but not in CD31⁻ cells (Figure 6F and Figure XVIB in the Data Supplement).

These experiments show that the downregulation of MIR503HG mouse homolog Gm28730 in PH is associated with EndMT and that human MIR503HG_2 overexpression can prevent the induction of mesenchymal markers in the lung endothelial compartment in response to EndMT-inducing stimuli in vivo.

Loss of MIR503HG Is Associated With EndMT in Human PAH

Blood outgrowth ECs derived from patients with PAH have been shown to recapitulate pulmonary EC dysfunction.[22] Based on the expression of endothelial and mesenchymal markers, we showed that blood outgrowth ECs derived from patients with PAH presented an EndMT-like phenotype compared to cells from control patients that was accompanied by a significant reduction of MIR503HG_3 and MIR503HG_5 expression (Figure 7A).

To determine the association between the loss of MIR503HG and vascular remodeling, we analyzed lung tissue sections from 3 patients with PAH and 3 control lungs, using in situ hybridization. In control lungs, MIR503HG expression was present throughout the vasculature (Figure 7B and 7C, Figures XVIIA, XVIIB, and XVIIIA in the Data Supplement). Conversely, in PAH lung vasculature, MIR503HG expression was detected in nonremodeled vessels but was absent from remodeled arterial vessels (Figure 7B and 7C, Figures XVIIC and XVIID and VXIII in the Data Supplement).

Together, this demonstrated that loss of MIR503HG is observed in patients with PAH in association with vascular remodeling.

MIR503HG Regulation of EndMT Is Mediated in Part by Polypyrimidine Tract Binding Protein 1

To study the MIR503HG mechanism of action, we performed an RNA pulldown assay using in vitro synthesized biotinylated MIR503HG_2 transcripts, which were captured on streptavidin beads and incubated with HUVEC extracts depleted from the cytosolic fraction (Figure 8A and Figure XIXA and XIXB in the Data Supplement). Proteomic analysis by mass spectrometry was used to identify 125 significantly enriched proteins bound to biotinylated MIR503HG_2 compared with an enhanced green fluorescent protein (eGFP) RNA control (Dataset IV in the Data Supplement). The top 2 enriched proteins (ranked based on fold change over control) were the RNA splicing regulatory protein PTBP1 (polypyrimidine tract binding protein 1) and the HNRNPA0 (heterogeneous nuclear ribonucleoprotein A0; Figure 8B). Interaction of MIR503HG_2 with either PTBP1 or HNRNPA0 was validated by reciprocal RNA immunoprecipitation. MIR503HG_2 RNA showed high and significant enrichment for PTBP1 and HNRNPA0 pulldown compared to an IgG control pulldown, whereas, in comparison, UBC mRNA showed a lower enrichment (Figure 8C).

To understand the consequences of MIR503HG interaction with PTBP1 and HNRNPA0 proteins, we analyzed PTBP1 and HNRNPA0 protein levels in MIR503HG knockdown samples. Upon MIR503HG depletion, we observed a significant downregulation of PTBP1 (Figure 8D) and HNRNPA0 (Figure XIXC in the Data Supplement). Similarly, PTBP1 protein downregulation also occurs in EndMT (Figure 8E), along with HNRNPA0 (Figure XIXD in the Data Supplement). To determine if PTBP1 or HNRNPA0 downregulation contributes to EndMT, we performed siRNA-mediated PTBP1 and HNRNPA0 knockdown in HUVEC (Figure XIXE and XIXF in the Data Supplement) and assessed EndMT markers after 7 days. Interestingly, PTBP1 depletion led to a significant decrease of PECAM1 as well as the upregulation of COL1A1 and ACTA2, although SNAI2 was unaffected (Figure 8F), without significantly affecting MIR503HG levels (Figure XIXG and XIXH in the Data Supplement). In contrast, HNRNPA0 depletion only led to a significant increase of ACTA2 (Figure 8F). Furthermore, we mined publicly available RNA-seq datasets from PTBP1 knockdown in HepG2 cells, a liver hepatocellular carcinoma with epithelial cell morphology, and compared the differentially expressed genes with LNT503 regulated genes. This revealed a significant overlap between genes negatively regulated by MIR503HG and PTBP1 (Figure XX in the Data Supplement), with 79 genes also upregulated during EndMT (Figure 8G). Of interest, the overlapping

Figure 6 Continued. homolog *Gm28730* expression in TdTomato⁺ cells isolated from normoxia/vehicle (n=8 mice) or SuHx mouse lung tissue (n=7). **D**, Strategy to assess the effect of human MIR503HG_2 overexpression in EndMT in SuHx PAH model. **E,** Human MIR503HG_2, MIR503HG mouse lncRNA homolog Gm28730 and **(F)** endothelial/mesenchymal marker expression in CD31⁺ lung cells isolated from SuHx mouse lung tissue following MIR503HG overexpression with lentivirus (LNT)_503HG or LNT_Control (LNT_503HG n=5, LNT_Control n=4). Relative quantification of real-time quantitative polymerase chain reaction normalized to 18S relative to Normoxia (**B** and **C**) or lentivirus control (LNT_CT; **E** and **F**). Statistical analysis of **B** and **C** was done using an unpaired 2-tailed *t* test except for Col1a1 (Collagen type I alpha 1 chain) expression, not following a normal distribution, analyzed using a Mann-Whitney test. **E** and **F** were analyzed using Iman and Conover nonparametric ranking followed by unpaired 2-tailed *t* test. CDH5 indicates cadherin 5; eNOS, endothelial NO synthase; FACS, fluorescence-activated cell sorting; LV, lentivirus; PH, pulmonary hypertension; and RQ, relative quantification.

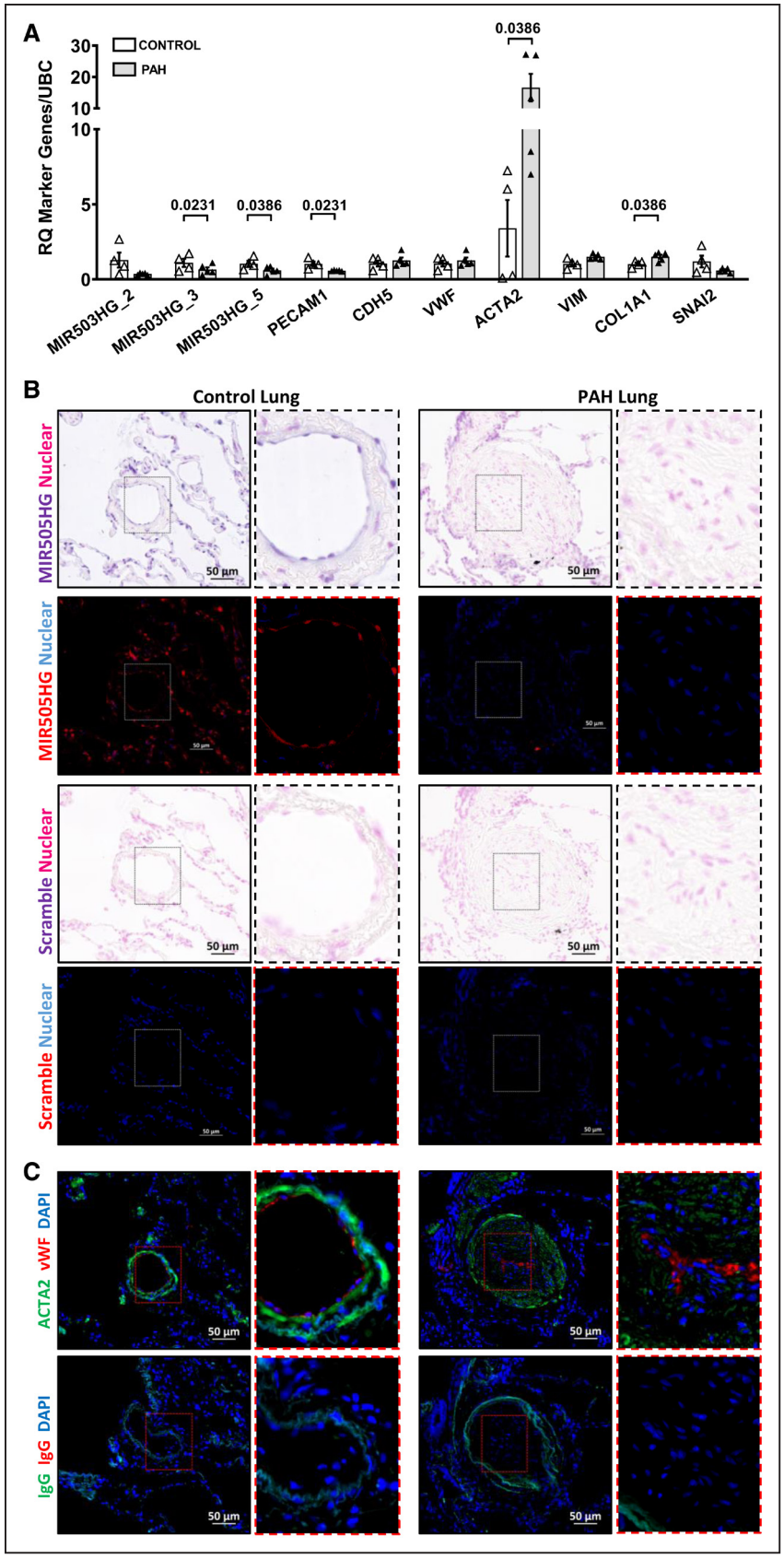

Figure 7. Human pulmonary arterial hypertension (PAH) is associated with loss of MIR503HG.
A, MIR503HG_2 and endothelial-to-mesenchymal transition (EndMT) markers gene expression in blood outgrowth endothelial cells isolated from patients with PAH and controls (control n=4, PAH n=5). Relative quantification of real-time quantitative polymerase chain reaction normalized to UBC (Ubiquitin C) relative to control cells. Analysis by Iman and Conover nonparametric ranking followed by unpaired 2-tailed *t* test. **B**, In situ hybridization for MIR503HG in control and PAH patient lungs, with brightfield staining, and pseudo fluorescence imaging to enhance visualization of MIR503HG (purple/red) and the nucleus (pink/blue). **C**, Immunofluorescence for smooth muscle cells (ACTA [α-smooth muscle actin] 2, green), endothelial cells (vWF [von Willebrand factor], red) and nucleus (DAPI [4′,6-diamidino-2-phenylindole], blue), and IgG controls in control and PAH patient lungs. Scale bar 50 µm. Dotted squares denote high-power view of vessels. CDH5 indicates cadherin 5; COL1A1, collagen type I alpha 1 chain; PECAM1, platelet endothelial cell adhesion molecule-1; RQ, relative quantification; SNAI2, snail family transcriptional repressor 2; and VIM, vimentin.

genes include several known mesenchymal markers: TAGLN, COL1A1, CNN1, VCAN, and MYL9. Altogether, these data suggest that the induction of EndMT by MIR503HG depletion may be mediated in part by a reduction in PTBP1 level and consequent upregulation of mesenchymal markers.

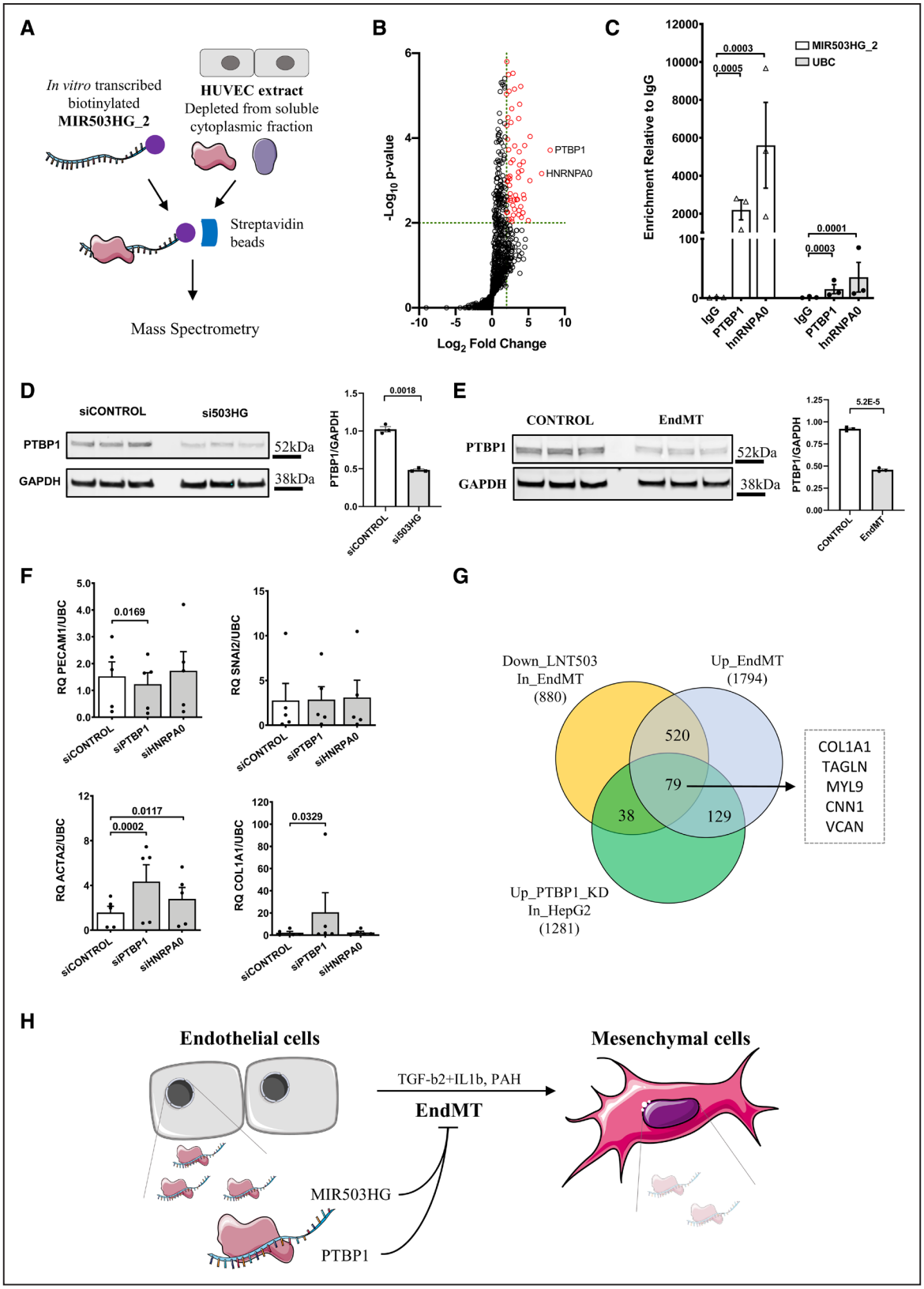

Figure 8. MIR503HG binding partner PTBP1 (polypyrimidine tract binding protein 1) regulates endothelial-to-mesenchymal transition (EndMT).

A, Schematic of MIR503HG in vitro pulldown experiment. **B**, Dot plot of −log10 *P* value vs log2 fold change of MIR503HG_2 interacting proteins compared to GFP (green fluorescent protein) control after RNA pulldown assay and mass spectrometry (n=3). **C**, Real-time quantitative polymerase chain reaction (RT-qPCR) analysis of MIR503HG_2 and UBC (Ubiquitin C) in RNA immunoprecipitation of IgG, PTBP1, and (*Continued*)

DISCUSSION

With the involvement of EndMT in pathological vascular remodeling,[11,23,24] the in-depth characterization of this process and its therapeutical targeting seems crucial. Here, we report the transcriptomic profile of primary EC undergoing EndMT in vitro using single-cell and bulk RNA-seq. We provide evidence of lncRNA expression changes associated with EndMT and the effect of the depletion of 4 candidate lncRNAs on EndMT. We have shown that loss of the lncRNA MIR503HG is pivotal to the induction of EndMT, both in vitro and in vivo, by a mechanism of action independent of miR-424 and miR-503. MIR503HG overexpression in PAH mice affects mesenchymal marker expression, highlighting potential for therapeutic intervention. Furthermore, MIR503HG loss was associated with human PAH, further confirming its clinical relevance. Our data revealed the interaction of MIR503HG with the RNA binding protein PTBP1 and suggests PTBP1 protein regulation by MIR503HG contributes to EndMT. A graphical summary of this mechanism is shown in Figure 8H.

EndMT has been observed in diseases affecting different vascular beds, from PAH[23,24] to atherosclerosis[25] and vein graft remodeling.[8,12] Although context-specific regulations of EndMT likely occur, common markers and pathways have been described.[1] Our data showing a large overlap of transcriptional changes between HUVEC and HPAEC undergoing EndMT support some common mechanisms, which could be targeted as a therapeutic strategy across diseases. Our work on MIR503HG revealed its relevance to EndMT in several EC types, 2 in vitro EndMT models, in a mouse model of PH, and in human PAH samples.

We propose that the TGF-β2 and IL-1β cotreatment model replicates an early stage of EndMT, as cotreated ECs still express the endothelial marker PECAM1 after 7 days, despite a significant downregulation of its expression. At this time point, we showed a decrease in cell proliferation and no statistical change in migration. Although fully transitioned cells have increased proliferative and migratory capacity,[12] this might not be the case for transitioning cells. Indeed, decreased proliferation has been observed in another in vitro EndMT model,[7,10] and similar phenotypes have been described previously in primary ECs upon activation of the TGF-β pathway.[26] Further work is required to characterize the different stages of EndMT, in terms of gene expression as well as cell phenotypic properties, both in vitro and in vivo.

MIR503HG was initially described as a hypoxia-sensitive lncRNA in EC[27] and several studies have independently focused on its role in cancer. Although MIR503HG generally inhibits cell proliferation, invasion, and migration in cancer cells,[19,28–31] except in lymphoma,[32] silencing of MIR503HG in ECs has been shown to decrease proliferation and migration,[27] corroborating our findings. These observations highlight the cell type–specific effect of lncRNA modulation. Our study is the first to provide evidence for the involvement of MIR503HG in EndMT.

Our study provides mechanistic data on MIR503HG, identifying binding partners in HUVEC. MIR503HG interaction with PTBP1 and HNRNPA0 was confirmed by reciprocal RNA immunoprecipitation. Several lncRNAs have been shown to interact with PTBP1, regulating its role in transcription,[33] splicing,[34] or RNA stability.[35] PTBP1 protein level was decreased in MIR503HG knockdown conditions and EndMT, suggesting MIR503HG interaction with PTBP1 in HUVEC may promote its stability. Knockdown of PTBP1 in HUVEC and HepG2 cells led to the upregulation of mesenchymal markers, showing PTBP1 plays a role in maintaining cell identity. The interaction of MIR503HG with HNRNPA2B1, observed in hepatocellular carcinoma,[31] was not detected in the HUVEC pulldown, suggesting cell type–specific mechanism of MIR503HG. Collectively, we propose that the role of MIR503HG in EndMT is mediated in part by its regulation of PTBP1 protein level.

Although miR-424 and miR-503 have roles in epithelial-to-mesenchymal transition,[36,37] our data shows that MIR503HG modulation, but not miRNA modulation, has an effect on the EndMT process. Indeed, CRISPR/Cas9–mediated deletion of the *MIR503HG* locus as well as MIR503HG transcript overexpression was sufficient to regulate EndMT, without affecting either miRNA expression. Crucially, targeted depletion of miR-503 and miR-424 did not show a statistical difference in the expression of EndMT markers. A decrease of miR-503 and miR-424 during EndMT or upon siRNA-mediated MIR503HG depletion is likely due to the overlap between the miRNA precursor and MIR503HG and their potential transcriptional coregulation. Although many miRNA host lncRNAs have been described, for the large part their function as independent lncRNAs, instead of primary miRNA transcripts, have not been determined, with the exception of MIR205HG/LEADeR[38] and MIR100HG.[39] LEADeR lncRNA is produced through splicing of the MIR205HG locus and regulates differentiation of human

Figure 8 Continued. HNRNPA0 (heterogeneous nuclear ribonucleoprotein A0) from human umbilical vein endothelial cells (HUVEC) lysate (n=3). **D**, Western blot analysis of PTBP1 level in si503HG (siRNA-mediated MIR503HG depleted) in HUVEC after 7 d. GAPDH used as a loading control. **E**, Western blot analysis of PTBP1 level in CONTROL and EndMT-HUVEC. GAPDH used as a loading control **(F)** EndMT marker expression in siPTBP1 (siRNA-mediated PTBP1 depleted) samples 7 d after transfection (n=5). **G**, Overlap of genes significantly downregulated by lentivirus (LNT)_503HG in EndMT condition, upregulated in EndMT compared to control and upregulated by PTBP1 in a human liver cancer cell line (HepG2). Relative quantification of RT-qPCR normalized to UBC relative to siCONTROL (siRNA control) treatment. Statistical analysis was done using a repeated-measures 1-way ANOVA with Bonferroni correction for **C** and **F** and linear mixed-effects modeling for **D** and **E**. ACTA2 indicates α-smooth muscle actin 2; COL1A1, collagen type I alpha 1 chain; IL, interleukin; KD, knockdown; PECAM1 indicates Platelet endothelial cell adhesion molecule-1; siHNRNPA0, siRNA-mediated HNRNPA0 depletion; SNAI2, snail family transcriptional repressor 2; PAH, pulmonary arterial hypertension; RQ, relative quantification; and TGF, transforming growth factor.

prostate basal cells independently of miR-205 function,[38] whereas MIR100HG regulates cell cycle through its interaction with the RNA binding protein HuR.[39] Our data provide another example of miRNA host gene with a long noncoding RNA role, highlighting the need to dissociate the effect of host genes from their overlapping miRNAs.

Our study also shows a clear correlation between loss of MIR503HG and the gain of EndMT markers, using a mouse model of PH and human blood outgrowth ECs. In PAH lung tissues, we showed the association between MIR503HG loss and vessel remodeling. Despite the semiquantitative analysis of the in situ hybridization presented, further in-depth studies are required to accurately establish a link between MIR503HG transcript levels and the extent of remodeling seen in PAH, as well as the contribution of EndMT in the context of human disease. Indeed, recent studies suggested the large contribution of smooth muscle cells and pericytes in the remodeling and lesions observed in PAH,[40,41] ultimately highlighting the multifactorial nature of the disease. It will also be of interest to assess if MIR503HG downregulation is relevant in other vascular remodeling pathologies associated with EndMT, such as atherosclerosis and vein graft failure.

Our data, showing a decrease of mesenchymal markers in mouse ECs after lentiviral delivery of human MIR503HG followed by SuHx model of PH, suggests MIR503HG plays a key role in the prevention of EndMT. The overexpression of miR-424/503 in the lung has previously been shown to prevent and rescue the SuHx PH phenotype in rats.[42] This suggests that MIR503HG and miR-424/503 may both contribute to PH but probably through different processes, supporting a partner relationship between miRNAs and their host gene.[43] Further studies, including normoxic control mice and optimized delivery strategies, are required to address the effect of MIR503HG on the severity of the PH phenotype. At present, the delivery of lncRNA to the EC compartment in vivo is too inefficient to justify such approaches.

Taken together, our comprehensive analysis has provided important insights into EndMT and highlighted the critical functional role of the lncRNA MIR503HG. Our results open new avenues for targeting EndMT in vascular remodeling, using lncRNA-directed therapeutics.

ARTICLE INFORMATION

Received September 17, 2020; revision received March 4, 2021; accepted March 9, 2021.

Affiliations

The Queen's Medical Research Institute, Centre for Cardiovascular Science (J.P.M., J.R., A. Caudrillier, J.P.S., A.-M.S., T.D., A.S., L. Deng, S.-H.C., K.S., A.T., T.M., J.I., P.W.F.H., L. Denby, A. Caporali, A.H.B.), Edinburgh Cancer Research UK Centre, Institute of Genetics and Molecular Medicine (A.v.K.), The Roslin Institute and Royal (Dick) School of Veterinary Studies (R.S.T.), and The Queen's Medical Research Institute, Centre for Inflammation Research (J.R.W.-K., N.C.H.), University of Edinburgh, Edinburgh, Scotland. Institute for Cardiovascular Physiology, Goethe University, Frankfurt, Germany (B.P.-M., M.S.L., R.P.B.). German Center of Cardiovascular Research (DZHK), Partner site RheinMain, Frankfurt, Germany (B.P.-M., M.S.L., R.P.B.). Institute of Cardiovascular and Medical Sciences, British Heart Foundation (BHF) Glasgow Centre, University of Glasgow, Glasgow, United Kingdom (J.D.M., A.C.B.). BHF Cambridge (CRE), University of Cambridge, Cambridge, United Kingdom (P.C., N.W.M.). The Zena and Michael A. Wiener Cardiovascular Institute, School of Medicine at Mount Sinai, New York, New York (J.C.K.). Victor Chang Cardiac Research Institute, Darlinghurst, Australia. (J.C.K.). Department of Biological Regulation, Weizmann Institute of Science, Rehovot, Israel (I.U.).

Acknowledgments

We thank G. Aitchison and K. Newton for their technical assistance. Flow cytometry data was generated with support from the QMRI Flow Cytometry and cell sorting facility, University of Edinburgh. Mass Spectrometry data were generated with support from the IGMM Mass Spectrometry Facility, University of Edinburgh. We thank the University of Edinburgh Bioresearch & Veterinary Services for exemplary animal husbandry.

Sources of Funding

A.H. Baker is supported by European Research Council 338991 VASMIR (European Research Council Advanced Grant 338991), British Heart Foundation (BHF) Chair and Programme grants (CH/11/2/28733 and RG/14/3/30706) and project grant PG/20/10347. A.v. Kriegsheim is supported by Wellcome Trust (Multi-user Equipment Grant, 208402/Z/17/Z). J.C. Kovacic is supported by US National Institutes of Health (R01HL130423, R01HL135093, R01HL148167-01A1). M.S. Leisegang and R.P. Brandes are supported by Deutsche Forschungsgemeinschaft (DFG Transregio TRR267, TP A04&A06, EXS2026 Cardiopulmonary Institute–CPI).

Disclosures

None.

Supplemental Materials

Major Resources Table
Dataset I EndMT RNAseq
Dataset II GoTerms EndMT
Dataset III LNT503 RNAseq
Dataset IV PD MassSpec
Online Data Supplement
Uncut Gel Blots
References 44–63

REFERENCES

1. Kovacic JC, Dimmeler S, Harvey RP, Finkel T, Aikawa E, Krenning G, Baker AH. Endothelial to mesenchymal transition in cardiovascular disease: JACC state-of-the-art review. *J Am Coll Cardiol.* 2019;73:190–209. doi: 10.1016/j.jacc.2018.09.089
2. Manavski Y, Lucas T, Glaser SF, Dorsheimer L, Günther S, Braun T, Rieger MA, Zeiher AM, Boon RA, Dimmeler S. Clonal expansion of endothelial cells contributes to ischemia-induced neovascularization. *Circ Res.* 2018;122:670–677. doi: 10.1161/CIRCRESAHA.117.312310
3. Chen PY, Simons M. When endothelial cells go rogue. *EMBO Mol Med.* 2016;8:1–2. doi: 10.15252/emmm.201505943
4. Dejana E, Hirschi KK, Simons M. The molecular basis of endothelial cell plasticity. *Nat Commun.* 2017;8:14361. doi: 10.1038/ncomms14361
5. Zeisberg EM, Tarnavski O, Zeisberg M, Dorfman AL, McMullen JR, Gustafsson E, Chandraker A, Yuan X, Pu WT, Roberts AB, et al. Endothelial-to-mesenchymal transition contributes to cardiac fibrosis. *Nat Med.* 2007;13:952–961. doi: 10.1038/nm1613
6. Hashimoto N, Phan SH, Imaizumi K, Matsuo M, Nakashima H, Kawabe T, Shimokata K, Hasegawa Y. Endothelial-mesenchymal transition in bleomycin-induced pulmonary fibrosis. *Am J Respir Cell Mol Biol.* 2010;43:161–172. doi: 10.1165/rcmb.2009-0031OC
7. Evrard SM, Lecce L, Michelis KC, Nomura-Kitabayashi A, Pandey G, Purushothaman KR, d'Escamard V, Li JR, Hadri L, Fujitani K, et al. Endothelial to mesenchymal transition is common in atherosclerotic lesions and is associated with plaque instability. *Nat Commun.* 2016;7:11853. doi: 10.1038/ncomms11853
8. Cooley BC, Nevado J, Mellad J, Yang D, St Hilaire C, Negro A, Fang F, Chen G, San H, Walts AD, et al. TGF-β signaling mediates endothelial-to-mesenchymal transition (EndMT) during vein graft remodeling. *Sci Transl Med.* 2014;6:227ra34. doi: 10.1126/scitranslmed.3006927
9. Stenmark KR, Fagan KA, Frid MG. Hypoxia-induced pulmonary vascular remodeling: cellular and molecular mechanisms. *Circ Res.* 2006;99:675–691. doi: 10.1161/01.RES.0000243584.45145.3f
10. Good RB, Gilbane AJ, Trinder SL, Denton CP, Coghlan G, Abraham DJ, Holmes AM. Endothelial to mesenchymal transition contributes to

endothelial dysfunction in pulmonary arterial hypertension. *Am J Pathol*. 2015;185:1850–1858. doi: 10.1016/j.ajpath.2015.03.019
11. Ranchoux B, Antigny F, Rucker-Martin C, Hautefort A, Péchoux C, Bogaard HJ, Dorfmüller P, Remy S, Lecerf F, Planté S, et al. Endothelial-to-mesenchymal transition in pulmonary hypertension. *Circulation*. 2015;131:1006–1018. doi: 10.1161/CIRCULATIONAHA.114.008750
12. Suzuki T, Carrier EJ, Talati MH, Rathinasabapathy A, Chen X, Nishimura R, Tada Y, Tatsumi K, West J. Isolation and characterization of endothelial-to-mesenchymal transition cells in pulmonary arterial hypertension. *Am J Physiol Lung Cell Mol Physiol*. 2018;314:L118–L126. doi: 10.1152/ajplung.00296.2017
13. Maleszewska M, Moonen JR, Huijkman N, van de Sluis B, Krenning G, Harmsen MC. IL-1β and TGFβ2 synergistically induce endothelial to mesenchymal transition in an NFκB-dependent manner. *Immunobiology*. 2013;218:443–454. doi: 10.1016/j.imbio.2012.05.026
14. Kumarswamy R, Volkmann I, Jazbutyte V, Dangwal S, Park DH, Thum T. Transforming growth factor-β-induced endothelial-to-mesenchymal transition is partly mediated by microRNA-21. *Arterioscler Thromb Vasc Biol*. 2012;32:361–369. doi: 10.1161/ATVBAHA.111.234286
15. Schmitz SU, Grote P, Herrmann BG. Mechanisms of long noncoding RNA function in development and disease. *Cell Mol Life Sci*. 2016;73:2491–2509. doi: 10.1007/s00018-016-2174-5
16. Monteiro JP, Bennett M, Rodor J, Caudrillier A, Ulitsky I, Baker AH. Endothelial function and dysfunction in the cardiovascular system: the long non-coding road. *Cardiovasc Res*. 2019;115:1692–1704. doi: 10.1093/cvr/cvz154
17. Xiang Y, Zhang Y, Tang Y, Li Q. MALAT1 modulates TGF-β1-induced endothelial-to-mesenchymal transition through downregulation of miR-145. *Cell Physiol Biochem*. 2017;42:357–372. doi: 10.1159/000477479
18. Neumann P, Jaé N, Knau A, Glaser SF, Fouani Y, Rossbach O, Krüger M, John D, Bindereif A, Grote P, et al. The lncRNA GATA6-AS epigenetically regulates endothelial gene expression via interaction with LOXL2. *Nat Commun*. 2018;9:237. doi: 10.1038/s41467-017-02431-1
19. Muys BR, Lorenzi JC, Zanette DL, Lima e Bueno Rde B, de Araújo LF, Dinarte-Santos AR, Alves CP, Ramão A, de Molfetta GA, Vidal DO, et al. Placenta-enriched LincRNAs MIR503HG and LINC00629 decrease migration and invasion potential of JEG-3 cell line. *PLoS One*. 2016;11:e0151560. doi: 10.1371/journal.pone.0151560
20. Sörensen I, Adams RH, Gossler A. DLL1-mediated Notch activation regulates endothelial identity in mouse fetal arteries. *Blood*. 2009;113:5680–5688. doi: 10.1182/blood-2008-08-174508
21. Monvoisin A, Alva JA, Hofmann JJ, Zovein AC, Lane TF, Iruela-Arispe ML. VE-cadherin-CreERT2 transgenic mouse: a model for inducible recombination in the endothelium. *Dev Dyn*. 2006;235:3413–3422. doi: 10.1002/dvdy.20982
22. Caruso P, Dunmore BJ, Schlosser K, Schoors S, Dos Santos C, Perez-Iratxeta C, Lavoie JR, Zhang H, Long L, Flockton AR, et al. Identification of MicroRNA-124 as a major regulator of enhanced endothelial cell glycolysis in pulmonary arterial hypertension via PTBP1 (polypyrimidine tract binding protein) and pyruvate kinase M2. *Circulation*. 2017;136:2451–2467. doi: 10.1161/CIRCULATIONAHA.117.028034
23. Ranchoux B, Harvey LD, Ayon RJ, Babicheva A, Bonnet S, Chan SY, Yuan JX, Perez VJ. Endothelial dysfunction in pulmonary arterial hypertension: an evolving landscape (2017 grover conference series). *Pulm Circ*. 2018;8:2045893217752912. doi: 10.1177/2045893217752912
24. Hopper RK, Moonen JR, Diebold I, Cao A, Rhodes CJ, Tojais NF, Hennigs JK, Gu M, Wang L, Rabinovitch M. In pulmonary arterial hypertension, reduced BMPR2 promotes endothelial-to-mesenchymal transition via HMGA1 and its target slug. *Circulation*. 2016;133:1783–1794. doi: 10.1161/CIRCULATIONAHA.115.020617
25. Chen PY, Qin L, Baeyens N, Li G, Afolabi T, Budatha M, Tellides G, Schwartz MA, Simons M. Endothelial-to-mesenchymal transition drives atherosclerosis progression. *J Clin Invest*. 2015;125:4514–4528. doi: 10.1172/JCI82719
26. Goumans MJ, Valdimarsdottir G, Itoh S, Rosendahl A, Sideras P, ten Dijke P. Balancing the activation state of the endothelium via two distinct TGF-beta type I receptors. *EMBO J*. 2002;21:1743–1753. doi: 10.1093/emboj/21.7.1743
27. Fiedler J, Breckwoldt K, Remmele CW, Hartmann D, Dittrich M, Pfanne A, Just A, Xiao K, Kunz M, Müller T, et al. Development of long noncoding RNA-based strategies to modulate tissue vascularization. *J Am Coll Cardiol*. 2015;66:2005–2015. doi: 10.1016/j.jacc.2015.07.081
28. Qiu F, Zhang MR, Zhou Z, Pu JX, Zhao XJ. lncRNA MIR503HG functioned as a tumor suppressor and inhibited cell proliferation, metastasis and epithelial-mesenchymal transition in bladder cancer. *J Cell Biochem*. 2019;120:10821–10829. doi: 10.1002/jcb.28373
29. Fu J, Dong G, Shi H, Zhang J, Ning Z, Bao X, Liu C, Hu J, Liu M, Xiong B. LncRNA MIR503HG inhibits cell migration and invasion via miR-103/OLFM4 axis in triple negative breast cancer. *J Cell Mol Med*. 2019;23:4738–4745. doi: 10.1111/jcmm.14344
30. Chuo D, Liu F, Chen Y, Yin M. LncRNA MIR503HG is downregulated in Han Chinese with colorectal cancer and inhibits cell migration and invasion mediated by TGF-β2. *Gene*. 2019;713:143960. doi: 10.1016/j.gene.2019.143960
31. Wang H, Liang L, Dong Q, Huan L, He J, Li B, Yang C, Jin H, Wei L, Yu C, et al. Long noncoding RNA miR503HG, a prognostic indicator, inhibits tumor metastasis by regulating the HNRNPA2B1/NF-κB pathway in hepatocellular carcinoma. *Theranostics*. 2018;8:2814–2829. doi: 10.7150/thno.23012
32. Huang PS, Chung IH, Lin YH, Lin TK, Chen WJ, Lin KH. The long noncoding rna mir503hg enhances proliferation of human alk-negative anaplastic large-cell lymphoma. *Int J Mol Sci*. 2018;19:1463. doi: 10.3390/ijms19051463
33. Lin N, Chang KY, Li Z, Gates K, Rana ZA, Dang J, Zhang D, Han T, Yang CS, Cunningham TJ, et al. An evolutionarily conserved long noncoding RNA TUNA controls pluripotency and neural lineage commitment. *Mol Cell*. 2014;53:1005–1019. doi: 10.1016/j.molcel.2014.01.021
34. Ramos AD, Andersen RE, Liu SJ, Nowakowski TJ, Hong SJ, Gertz C, Salinas RD, Zarabi H, Kriegstein AR, Lim DA. The long noncoding RNA Pnky regulates neuronal differentiation of embryonic and postnatal neural stem cells. *Cell Stem Cell*. 2015;16:439–447. doi: 10.1016/j.stem.2015.02.007
35. Li J, Yang Y, Fan J, Xu H, Fan L, Li H, Zhao RC. Long noncoding RNA ANCR inhibits the differentiation of mesenchymal stem cells toward definitive endoderm by facilitating the association of PTBP1 with ID2. *Cell Death Dis*. 2019;10:492. doi: 10.1038/s41419-019-1738-3
36. Drasin DJ, Guarnieri AL, Neelakantan D, Kim J, Cabrera JH, Wang CA, Zaberezhnyy V, Gasparini P, Cascione L, Huebner K, et al. TWIST1-Induced miR-424 reversibly drives mesenchymal programming while inhibiting tumor initiation. *Cancer Res*. 2015;75:1908–1921. doi: 10.1158/0008-5472.CAN-14-2394
37. Yan W, Wu Q, Yao W, Li Y, Liu Y, Yuan J, Han R, Yang J, Ji X, Ni C. MiR-503 modulates epithelial-mesenchymal transition in silica-induced pulmonary fibrosis by targeting PI3K p85 and is sponged by lncRNA MALAT1. *Sci Rep*. 2017;7:11313. doi: 10.1038/s41598-017-11904-8
38. Profumo V, Forte B, Percio S, Rotundo F, Doldi V, Ferrari E, Fenderico N, Dugo M, Romagnoli D, Benelli M, et al. LEADeR role of miR-205 host gene as long noncoding RNA in prostate basal cell differentiation. *Nat Commun*. 2019;10:307. doi: 10.1038/s41467-018-08153-2
39. Sun Q, Tripathi V, Yoon JH, Singh DK, Hao Q, Min KW, Davila S, Zealy RW, Li XL, Polycarpou-Schwarz M, et al. MIR100 host gene-encoded lncRNAs regulate cell cycle by modulating the interaction between HuR and its target mRNAs. *Nucleic Acids Res*. 2018;46:10405–10416. doi: 10.1093/nar/gky696
40. Steffes LC, Froistad AA, Andruska A, Boehm M, McGlynn M, Zhang F, Zhang W, Hou D, Tian X, Miquerol L, et al. A notch3-marked subpopulation of vascular smooth muscle cells is the cell of origin for occlusive pulmonary vascular lesions. *Circulation*. 2020;142:1545–1561. doi: 10.1161/CIRCULATIONAHA.120.045750
41. Bordenave J, Tu L, Berrebeh N, Thuillet R, Cumont A, Le Vely B, Fadel E, Nadaud S, Savale L, Humbert M, et al. Lineage tracing reveals the dynamic contribution of pericytes to the blood vessel remodeling in pulmonary hypertension. *Arterioscler Thromb Vasc Biol*. 2020;40:766–782. doi: 10.1161/ATVBAHA.119.313715
42. Kim J, Kang Y, Kojima Y, Lighthouse JK, Hu X, Aldred MA, McLean DL, Park H, Comhair SA, Greif DM, et al. An endothelial apelin-FGF link mediated by miR-424 and miR-503 is disrupted in pulmonary arterial hypertension. *Nat Med*. 2013;19:74–82. doi: 10.1038/nm.3040
43. Gao X, Qiao Y, Han D, Zhang Y, Ma N. Enemy or partner: relationship between intronic micrornas and their host genes. *IUBMB Life*. 2012;64:835–840. doi: 10.1002/iub.1079
44. Haeussler M, Schönig K, Eckert H, Eschstruth A, Mianné J, Renaud JB, Schneider-Maunoury S, Shkumatava A, Teboul L, Kent J, et al. Evaluation of off-target and on-target scoring algorithms and integration into the guide RNA selection tool CRISPOR. *Genome Biol*. 2016;17:148. doi: 10.1186/s13059-016-1012-2
45. Sanjana NE, Shalem O, Zhang F. Improved vectors and genome-wide libraries for CRISPR screening. *Nat Methods*. 2014;11:783–784. doi: 10.1038/nmeth.3047
46. Mahmoud AD, Ballantyne MD, Miscianinov V, Pinel K, Hung J, Scanlon JP, Iyinikkel J, Kaczynski J, Tavares AS, Bradshaw AC, et al. The human-specific and smooth muscle cell-enriched LncRNA SMILR promotes proliferation by

regulating mitotic CENPF mRNA and drives cell-cycle progression which can be targeted to limit vascular remodeling. *Circ Res*. 2019;125:535–551. doi: 10.1161/CIRCRESAHA.119.314876

47. Dobin A, Davis CA, Schlesinger F, Drenkow J, Zaleski C, Jha S, Batut P, Chaisson M, Gingeras TR. STAR: ultrafast universal RNA-seq aligner. *Bioinformatics*. 2013;29:15–21. doi: 10.1093/bioinformatics/bts635
48. Li B, Dewey CN. RSEM: accurate transcript quantification from RNA-Seq data with or without a reference genome. *BMC Bioinformatics*. 2011;12:323. doi: 10.1186/1471-2105-12-323
49. Love MI, Huber W, Anders S. Moderated estimation of fold change and dispersion for RNA-seq data with DESeq2. *Genome Biol*. 2014;15:550. doi: 10.1186/s13059-014-0550-8
50. Robinson MD, McCarthy DJ, Smyth GK. edgeR: a Bioconductor package for differential expression analysis of digital gene expression data. *Bioinformatics*. 2010;26:139–140. doi: 10.1093/bioinformatics/btp616
51. Rajkumar AP, Qvist P, Lazarus R, Lescai F, Ju J, Nyegaard M, Mors O, Børglum AD, Li Q, Christensen JH. Experimental validation of methods for differential gene expression analysis and sample pooling in RNA-seq. *BMC Genomics*. 2015;16:548. doi: 10.1186/s12864-015-1767-y
52. Butler A, Hoffman P, Smibert P, Papalexi E, Satija R. Integrating single-cell transcriptomic data across different conditions, technologies, and species. *Nat Biotechnol*. 2018;36:411–420. doi: 10.1038/nbt.4096
53. Pitulescu ME, Schmidt I, Giaimo BD, Antoine T, Berkenfeld F, Ferrante F, Park H, Ehling M, Biljes D, Rocha SF, et al. Dll4 and Notch signalling couples sprouting angiogenesis and artery formation. *Nat Cell Biol*. 2017;19:915–927. doi: 10.1038/ncb3555
54. Madisen L, Zwingman TA, Sunkin SM, Oh SW, Zariwala HA, Gu H, Ng LL, Palmiter RD, Hawrylycz MJ, Jones AR, et al. A robust and high-throughput Cre reporting and characterization system for the whole mouse brain. *Nat Neurosci*. 2010;13:133–140. doi: 10.1038/nn.2467
55. Naeije R, D'Alto M. Sex matters in pulmonary arterial hypertension. *Eur Respir J*. 2014;44:553–554. doi: 10.1183/09031936.00054514
56. Al-Naamani N, Ventetuolo CE. Another piece in the estrogen puzzle of pulmonary hypertension. *Am J Respir Crit Care Med*. 2020;201:274–275. doi: 10.1164/rccm.201910-1982ED
57. Wallace E, Morrell NW, Yang XD, Long L, Stevens H, Nilsen M, Loughlin L, Mair KM, Baker AH, MacLean MR. A sex-specific MicroRNA-96/5-hydroxytryptamine 1B axis influences development of pulmonary hypertension. *Am J Respir Crit Care Med*. 2015;191:1432–1442. doi: 10.1164/rccm.201412-2148OC
58. Deng L, Blanco FJ, Stevens H, Lu R, Caudrillier A, McBride M, McClure JD, Grant J, Thomas M, Frid M, et al. MicroRNA-143 activation regulates smooth muscle and endothelial cell crosstalk in pulmonary arterial hypertension. *Circ Res*. 2015;117:870–883. doi: 10.1161/CIRCRESAHA.115.306806
59. Vitali SH, Hansmann G, Rose C, Fernandez-Gonzalez A, Scheid A, Mitsialis SA, Kourembanas S. The Sugen 5416/hypoxia mouse model of pulmonary hypertension revisited: long-term follow-up. *Pulm Circ*. 2014;4:619–629. doi: 10.1086/678508
60. Fehrenbach ML, Cao G, Williams JT, Finklestein JM, Delisser HM. Isolation of murine lung endothelial cells. *Am J Physiol Lung Cell Mol Physiol*. 2009;296:L1096–L1103. doi: 10.1152/ajplung.90613.2008
61. Humbert M, Guignabert C, Bonnet S, Dorfmüller P, Klinger JR, Nicolls MR, Olschewski AJ, Pullamsetti SS, Schermuly RT, Stenmark KR, et al. Pathology and pathobiology of pulmonary hypertension: State of the art and research perspectives. *Eur Respir J*. 2019;53:1801887. doi: 10.1183/13993003.01887-2018
62. Baghirova S, Hughes BG, Hendzel MJ, Schulz R. Sequential fractionation and isolation of subcellular proteins from tissue or cultured cells. *MethodsX*. 2015;2:440–445. doi: 10.1016/j.mex.2015.11.001
63. Livak KJ, Schmittgen TD. Analysis of relative gene expression data using real-time quantitative PCR and the 2(-Delta Delta C(T)) Method. *Methods*. 2001;25:402–408. doi: 10.1006/meth.2001.1262